

# Dalton Transactions

Accepted Manuscript



This article can be cited before page numbers have been issued, to do this please use: R. L. Hollingsworth, A. Bheemaraju, N. Lenca, R. L. Lord and S. Groyzman, *Dalton Trans.*, 2017, DOI: 10.1039/C6DT04532D.



This is an Accepted Manuscript, which has been through the Royal Society of Chemistry peer review process and has been accepted for publication.

Accepted Manuscripts are published online shortly after acceptance, before technical editing, formatting and proof reading. Using this free service, authors can make their results available to the community, in citable form, before we publish the edited article. We will replace this Accepted Manuscript with the edited and formatted Advance Article as soon as it is available.

You can find more information about Accepted Manuscripts in the [author guidelines](#).

Please note that technical editing may introduce minor changes to the text and/or graphics, which may alter content. The journal's standard [Terms & Conditions](#) and the ethical guidelines, outlined in our [author and reviewer resource centre](#), still apply. In no event shall the Royal Society of Chemistry be held responsible for any errors or omissions in this Accepted Manuscript or any consequences arising from the use of any information it contains.

## Divergent Reactivity of a New Dinuclear Xanthene-Bridged Bis(iminopyridine) Di-Nickel Complex with Alkynes

Ryan L. Hollingsworth,<sup>1</sup> Amarnath Bheemaraju,<sup>1,2</sup> Nicole Lenca,<sup>3</sup> Richard L. Lord,<sup>\*4</sup> Stanislav Groysman<sup>\*1</sup>

<sup>1</sup>Department of Chemistry, Wayne State University, 5101 Cass Ave, Detroit, MI, 48202.

<sup>2</sup>Current Address: BML Munjal University, 7th KM Stone, NH-8, Gurgaon, Haryana, India

<sup>3</sup>Lumigen Instrument Center, Department of Chemistry, Wayne State University, 5101 Cass Ave, Detroit, MI, 48202. <sup>2</sup>Department of Chemistry, Grand Valley State University, Allendale, MI, 49401.

\*E-mail: [groysman@chem.wayne.edu](mailto:groysman@chem.wayne.edu), [lordri@gvsu.edu](mailto:lordri@gvsu.edu)

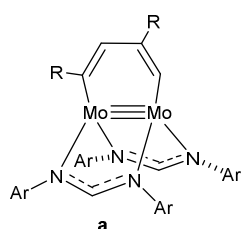
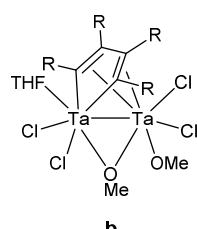
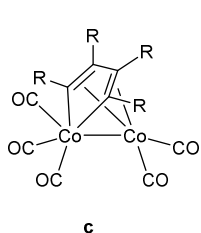
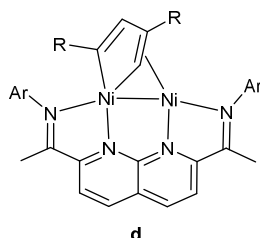
## Abstract

The reaction of a dinucleating bis(iminopyridine) ligand L bearing a xanthene linker (L = N,N'-(2,7-di-tert-butyl-9,9-dimethyl-9H-xanthene-4,5-diyl)bis(1-(pyridin-2-yl)methanimine)) with  $\text{Ni}_2(\text{COD})_2(\text{DPA})$  (COD = cyclooctadiene, DPA = diphenylacetylene) leads to the formation of a new dinuclear complex  $\text{Ni}_2(\text{L})(\text{DPA})$ .  $\text{Ni}_2(\text{L})(\text{DPA})$  can be also obtained in a one-pot reaction involving  $\text{Ni}(\text{COD})_2$ , DPA and L. The X-ray structure of  $\text{Ni}_2(\text{L})(\text{DPA})$  reveals two square-pyramidal Ni centers bridged by a DPA ligand. DFT calculations suggest this species features  $\text{Ni}^{\text{I}}$  centers antiferromagnetically coupled to each other and their iminopyridine ligand radicals. Treatment of  $\text{Ni}_2(\text{L})(\text{DPA})$  with one equivalent of ethyl propiolate ( $\text{HCCCO}_2\text{Et}$ ) forms the  $\text{Ni}_2(\text{L})(\text{HCCCO}_2\text{Et})$  complex. Addition of the second equivalent of ethyl propiolate leads to the observation of cyclotrimerised products by  $^1\text{H}$  NMR spectroscopy. Carrying out the reaction under catalytic conditions (1 mol% of  $\text{Ni}_2(\text{L})(\text{DPA})$ , 24 h, room temperature) transforms 89% of the substrate, forming primarily benzene products (triethyl benzene-1,3,5-tricarboxylate and triethyl benzene-1,2,4-tricarboxylate) in 68% yield, in ca. 5:1 relative ratio. Increasing catalyst loading to 5 mol% leads to the full conversion of ethyl propiolate to benzene products; no cyclotetramerisation products were observed. In contrast, the reaction is significantly more sluggish with methyl propargyl ether. Using 1 mol% of the catalyst, only 25% conversion of methyl propargyl ether was observed within 24 h at room temperature. Furthermore, methyl propargyl ether demonstrates formation of cyclooctatetraenes in significant amounts at low catalyst concentration, whereas higher catalyst concentration (5 mol%) leads to benzene products exclusively. Density functional theory was used to provide insight into the reaction mechanism, including structures of putative dinuclear metallocyclopentadiene and metallocycloheptatriene intermediates.

## Introduction

Transition metal-catalyzed cyclotrimerisation of mono-substituted alkynes is a well-studied transformation that yields a variety of aromatic compounds.<sup>1, 2</sup> Several factors are of importance in cyclotrimerisation, including regioselectivity (ratio of 1,3,5- to 1,2,4-isomers), and the overall selectivity of the cyclotrimerised product versus larger-size rings (generally cyclooctatetraenes) and/or oligomers.<sup>1</sup> Cyclotrimerisation is generally proposed to involve oxidative coupling as the first step to give metallacyclopentadiene.<sup>1,2</sup> Subsequent [4+2] cycloaddition yields the resulting substituted benzene.<sup>2</sup> An alternative mechanism for the second step involves alkyne insertion into a metal-carbon bond to give metallacycloheptatriene, which may undergo reductive elimination/cyclization to give benzene; this mechanism may explain formation of observed by-products such as large-size rings.<sup>3</sup> Many different monometallic precursors serve as precatalysts for cycloaddition of alkynes, including various nickel complexes.<sup>4</sup> In recent years, there has been a growing interest in pre-designed bimetallics for cyclotrimerisation.<sup>5</sup> Similar to the case of mononuclear catalysts, metallacyclopentadiene is proposed to serve as the key intermediate in cyclotrimerisation.<sup>5</sup> In contrast to the mononuclear complexes, such metallacyclopentadiene is likely to bind to both metals, which may have a significant impact on reactivity and selectivity of the catalyst.<sup>5</sup> However, the bridging metalocyclopentadiene structure is far from uniform in these complexes (**Figure 1, a-d**), depending on the distance between the metals and the nature of the metal centers.<sup>5</sup> Most of the previously reported bimetallics for cyclotrimerisation involved early transition metals,<sup>5-10</sup> whereas the use of late transition metal dinuclear complexes for alkyne trimerisation is relatively uncommon.<sup>5, 11</sup> In most of the previously reported cases, dinuclear complexes under investigation were assembled with an aid of a bridging monodentate ligand (OMe, Cl) or by a direct metal-

metal bond (W=W) prior to the reaction with alkynes. The lack of a stabilising dinucleating ligand that secures a relatively fixed metal-metal distance may lead to lower stability within the catalyst, enabling decomposition into mononuclear species. Uyeda and coworkers have recently reported a di-nickel complex, supported by a dinucleating ligand, that serves as highly effective and selective catalyst for cyclotrimerisation of terminal alkynes (**Figure 1, d**).<sup>13</sup> It is possible that the key to the outstanding performance of Uyeda's catalyst lies in the fact that the ligand utilized was highly rigid, fixing the nickels at a specific distance from each other, in a sharp contrast to the related mononuclear complexes that form mixtures of benzenes and cyclooctatetraenes.<sup>13</sup> Our group is investigating cooperative reactivity of late base transition metal complexes in the activation of small molecules and catalysis.<sup>14</sup> Following Uyeda's report, we became interested in the effect of nickel-nickel distance and overall ligand flexibility on cyclotrimerisation reactivity. Herein we report synthesis, structure, and cyclotrimerisation reactivity of a new di-nickel complex ligated by a semi-rigid dinucleating ligand, featuring two iminopyridine chelates brought together by a xanthene bridge (Scheme 1).

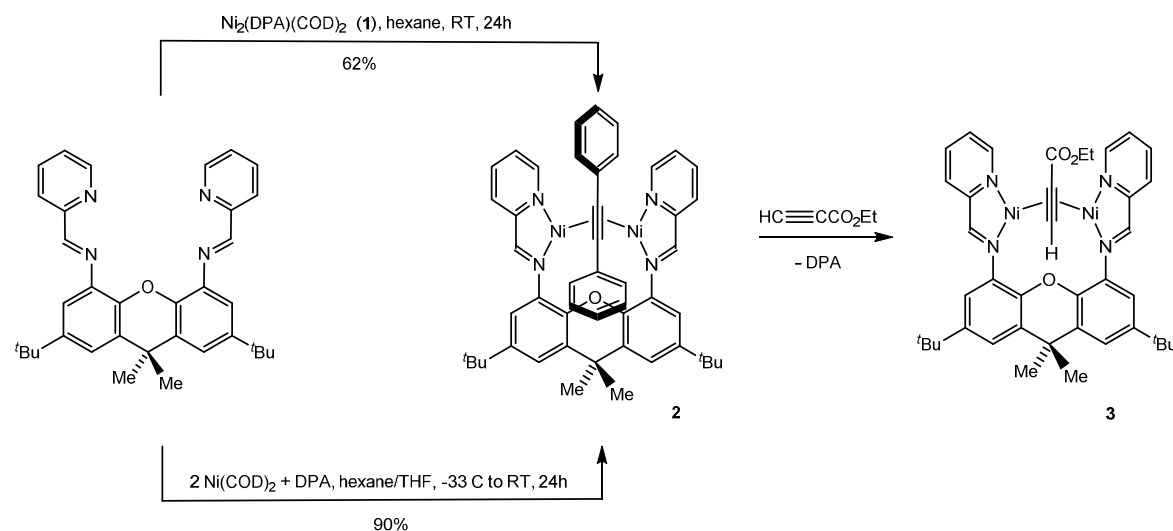
Tsai and coworkers<sup>10</sup>Mashima and coworkers<sup>9</sup>Knox, Spicer and coworkers<sup>12</sup>Uyeda and coworkers<sup>13</sup>

**Figure 1.** The structures of bridging metallocyclopentadiene intermediate in selected bimetallics.

## Results and Discussion

### Synthesis and Characterization Dinickel-Alkyne Complex

Our initial attempt to synthesize low-valent dinickel complex with L involved treatment of two equivalents of  $\text{Ni}(\text{COD})_2$  with one equivalent of L.  $^1\text{H}$  NMR of the crude product suggested formation of the bis(homoleptic) complex  $\text{NiL}_2$ , along with unreacted  $\text{Ni}(\text{COD})_2$ . Next, we turned our attention to the preformed di-nickel precursor  $\text{Ni}_2(\text{COD})_2(\text{DPA})$  (**1**) (COD = cyclooctadiene, DPA = diphenylacetylene) originally reported by Muetterties and coworkers.<sup>15</sup> Treatment of **1** with one equivalent of L generates a dinuclear complex  $\text{Ni}_2(\text{L})(\text{DPA})$  (**2**). Complex **2** is isolated in 62% yield as black crystalline solid. Prior isolation of precursor **1** turned out to be unnecessary: a combination of two equivalents of  $\text{Ni}(\text{COD})_2$ , one equivalent of DPA and one equivalent of L forms complex **2** in 90% isolated yield.



**Scheme 1.** Reaction pathways leading to compounds **2** and **3**.

Complex **2** was characterized by  $^1\text{H}$  and  $^{13}\text{C}$  NMR spectroscopy, X-ray crystallography and elemental analysis. The NMR spectrum of **2** indicated a  $C_s$ -symmetrical structure. Thus, imino protons give rise to one singlet at 9.50 ppm, while the t-butyl groups appear as a sharp singlet at 1.37 ppm. In contrast, the xanthene methyl groups give rise to two singlets integrating as three protons each, at 1.62 ppm and 2.02 ppm. The solid-state structure of compound **2** is given in **Figure 2**. The structure demonstrates two square-planar nickel centers bridged by a diphenylacetylene ligand. The C-C bond distance of 1.369(4) Å in the bridging diphenylacetylene ligand indicates strong activation as a result of interaction with two reducing metal centers. This bond distance is comparable to the bridging diphenylacetylene bond distance of 1.386(11) Å in  $\text{Ni}_2(\text{DPA})(\text{COD})_2$ .<sup>15</sup> For comparison, we have recently reported a structure of a square-planar mononuclear  $\text{Ni}(\text{iminopyridine})(\text{DPA})$  complex, in which the acetylene CC bond of diphenylacetylene was determined to be 1.292(3) Å.<sup>16</sup> Bond metrics of the redox-active iminopyridine chelates also indicate a significant degree of reduction (see **Figure 2** for selected bond distances). Furthermore, Ni---Ni separation of 2.451(1) Å in **2** is shorter than the postulated single Ni-Ni bond (2.617(2) Å) in  $\text{Ni}_2(\text{DPA})(\text{COD})_2$ .<sup>14</sup> The iminopyridine bond lengths suggest a Ni(I) center,<sup>14a, b</sup> but the approximate square planar geometry at each metal suggests low-spin Ni(II). To better understand the electronic structure of this complex, we interrogated these species with density functional theory.

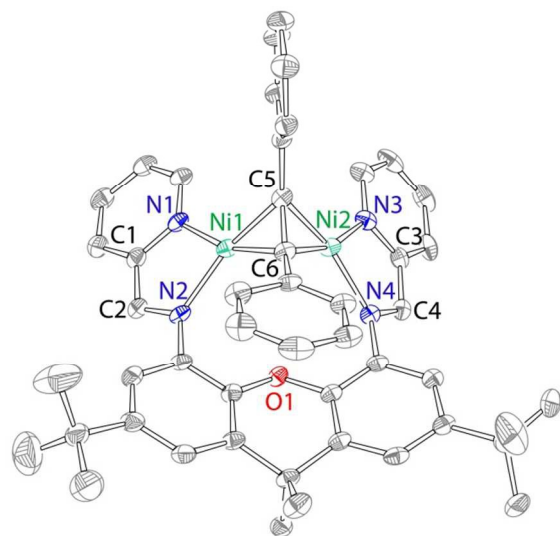


**Figure 2.** X-ray structure (50% ellipsoids) of complex **2**. H atoms and co-crystallized solvents (hexane and ether) are omitted for clarity. Selected bond distances: Ni1---Ni2 2.451(1) Å, Ni1 – C5 1.913(3) Å, Ni1 – C6 1.907(3) Å, Ni2 – C5 1.906(3) Å, Ni2 – C6 1.895(3) Å, C5 – C6 1.369(4) Å, N2 – C2 1.310(4) Å, N4 – C4 1.318(4) Å, C1 – C2 1.431(4) Å, C3 – C4 1.427(4) Å.

The geometry of a model mono-acetylene adduct (**4**) was optimized at the B3LYP/6-31G(d) level of theory.<sup>17</sup> t-Bu and Me substituents on the xanthene were truncated to H. The electronic structure of this optimized species is best described as an open-shell singlet with two Ni<sup>I</sup> ions antiferromagnetically coupled to both their iminopyridine ligands and the adjacent Ni center, as shown in the corresponding orbital analysis in **Figure 3**.<sup>18</sup> A simpler metric that further supports this interpretation is Mulliken spins of 0.80 and –0.80 for the two Ni centers. We find no evidence for covalent bonding between the two Ni centers; each bonding interaction is nullified by the appropriate antibonding combination (**Figure 3**).

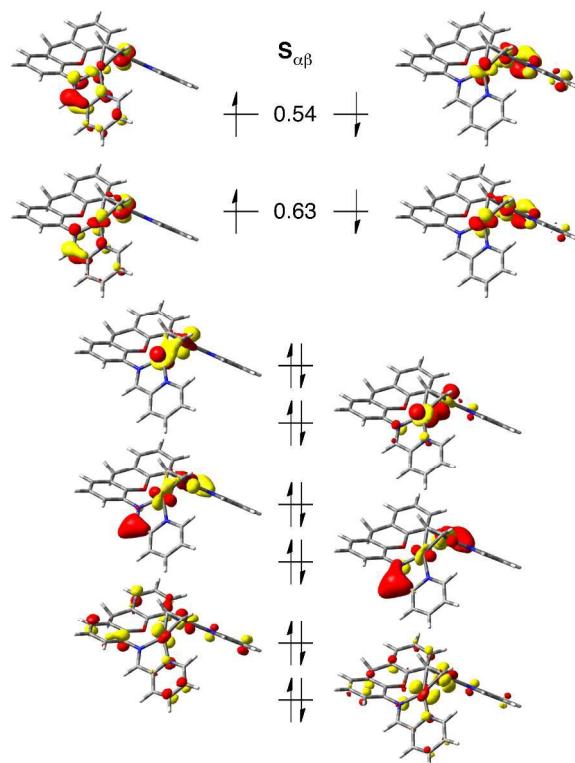


**Figure 3.** Corresponding orbitals with significant d-orbital character for **4**. Overlaps are listed for magnetically coupled orbitals. Images generated with GaussView.<sup>19</sup>

Consistent with a Ni<sup>I</sup> ion are iminopyridine bond lengths of 1.339, 1.420, and 1.380 Å for N<sub>im</sub>–C<sub>im</sub>, C<sub>im</sub>–C<sub>py</sub>, and C<sub>py</sub>–N<sub>py</sub>, respectively.<sup>15a, 15b, 20</sup> Significant activation of the alkyne is predicted with C–C elongation from 1.205 Å in free acetylene to 1.370 Å and deviation of the H–C–C angles from linear to ~140°. The optimized structure of **4** is shown in **Figure 4** along with mono-alkyne adducts (with the truncated xanthene backbone) of diphenylacetylene (**2'**), methyl propiolate (**5**), and methyl propargyl ether (**6**) (*vide infra*). The bond lengths in **2'** are in good agreement with those in **Figure 2**, deviating by only 0.02 Å.

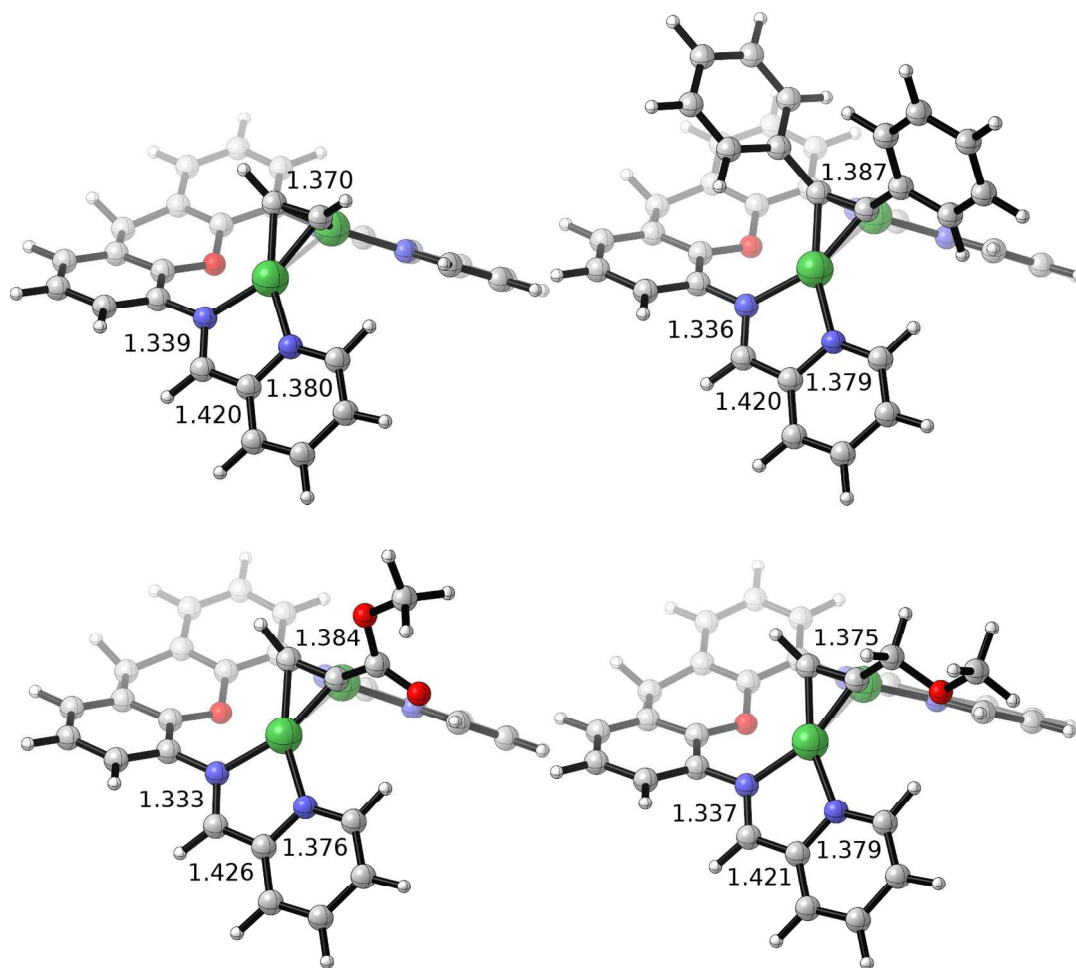


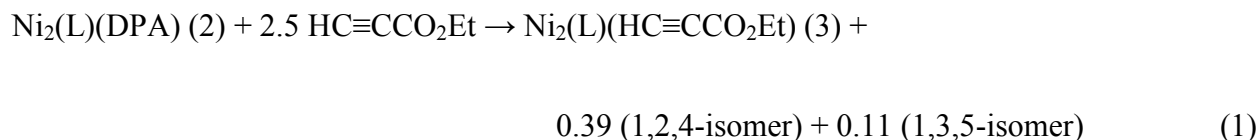
**Figure 4.** Comparison of the optimized geometries of **4** (top left), **2'** (top right), **5** (bottom left), and **6** (bottom right). Important bond lengths are listed in Å. Images generated in CYLview.<sup>21</sup>

Species **2'**, **5**, and **6** have similar electronic structures as **4**, as demonstrated by Mulliken spins of 0.74/−0.74, 0.66/−0.66, and 0.76/−0.76 for the Ni ions in these species. The iminopyridine bonding is also consistent with an iminosemiquinone form, as shown in Figure 2, with  $N_{im}-C_{im}$  bond lengths of 1.33–1.34 Å,  $C_{im}-C_{py}$  bond lengths of 1.42–1.43 Å, and  $C_{py}-N_{py}$  bond lengths of ~1.38 Å. Significant C–C activation is observed for each species with elongation from 1.216 to 1.387 Å for **2'**, 1.207 to 1.384 Å for **5**, and 1.206 to 1.375 Å for **6**. For the latter two species, structural data is only presented for the lowest energy regioisomer (see Figures S46

and S47). Collectively, these data suggest that regardless of the alkyne's nature, these species are all dinickel(I) and poised to undergo oxidative cyclization.

### Reactivity of Complex **2** with Alkynes

To determine whether complex **2** can serve as an appropriate pre-catalyst for cyclotrimerisation, its stoichiometric reactivity with two different terminal alkynes, ethyl propiolate and methyl propargyl ether, was evaluated. Addition of one equivalent of ethyl propiolate to **2** at room temperature forms complex **3** quantitatively, along with free diphenylacetylene. Complex **3** features similar spectroscopic features to those of **2**, indicating a similar structure. We were not able to obtain X-ray quality crystals of compound **3**, however, the DFT-optimized model **5** (with truncated xanthene backbone, *vide supra*) also indicates structure similar to that of **2**. Addition of the second equivalent of ethyl propiolate to **3** leads to full turnover: proton NMR of the reaction mixture demonstrates formation of (mostly) the respective 1,2,4-benzene product, along with complex **3**. Conducting the reaction of **2** with 2.5 equivalents of ethyl propiolate in the presence of an internal standard indicates reaction stoichiometry as shown in eq. 1. These findings indicate that “metallacyclopentadiene” intermediate is not stable in our system, unlike previously reported systems,<sup>5, 13</sup> and cannot be isolated. *However, the restoration of alkyne-bridged **3** following catalytic cycle supports the notion that the dinuclear nature of [Ni<sub>2</sub>(L)] remains intact throughout catalysis. For methyl propargyl ether, addition of one or two equivalents of the alkyne to the C<sub>6</sub>D<sub>6</sub> solution of **2** produces a mixture of compounds, which includes small amount of cyclotrimerisation products, along with additional unidentified compounds (see SI). It is important to emphasize that free ligand<sup>14f</sup> is not observed in any of these experiments, suggesting that [Ni<sub>2</sub>(L)] complexes do not decompose under these conditions.*



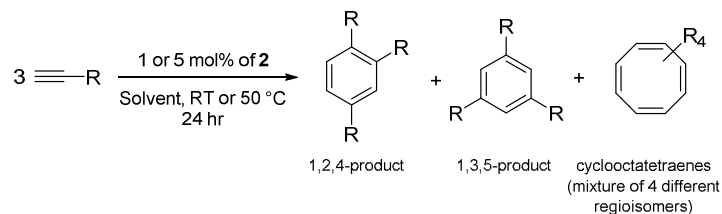
Next, we turned to investigate catalytic performance of complex **2** in cyclotrimerisation of various terminal alkynes. The results are summarized in **Table 1**. Varying reaction conditions were evaluated, including different catalyst loadings (1 or 5 mol%), different solvents ( $\text{C}_6\text{D}_6$ /ether/THF/ $\text{CH}_3\text{CN}$ ), and/or different reaction temperatures (RT or 50 °C); all experiments were run for 24 h. The degree of conversion of the alkyne substrates was determined by  $^1\text{H}$  NMR spectroscopy using an internal standard, hexamethylbenzene. The respective amounts of cyclotrimerised and cyclotetramerised products were elucidated using  $^1\text{H}$  NMR spectroscopy (by comparison to previously reported spectra),<sup>13, 22, 23</sup> or by GC-MS. As the first five entries in **Table 1** indicate, complex **2** catalyzes efficiently cyclotrimerisation of two different propiolates, ethyl and t-butyl. At low catalyst concentrations (1 mol%) in non-coordinating solvent ( $\text{C}_6\text{D}_6$ ), high conversion ( $\geq 90\%$ ) of the starting alkyne is obtained. Under these reaction conditions, cyclotrimerisation is not the sole reaction outcome: approximately 25-30% of the observed product is cyclooctatetraenes. Coordinating solvents (ethers or acetonitrile) have a negative effect on the overall cycloaddition reactivity. Increasing catalyst loading to 5 mol% leads to cyclotrimerisation exclusively for both propiolate substrates. Among the two possible benzene products, this system demonstrates good selectivity for the 1,2,4-isomer in  $\text{C}_6\text{D}_6$ .

With phenylacetylene, complex **2** forms benzene products exclusively, albeit less efficiently (compared to propiolates). At 1 mol%, approximately 30% conversion is observed at RT within 24 h, with 3:1 selectivity for 1,2,4-triphenylbenzene. Conversion can be increased by

increasing the amount of catalyst (from 1 to 5 mol%) and further by increasing reaction temperature (to 92% total). Significantly, increasing catalyst loading and reaction temperature maintains 3:1 ratio of the obtained 1,2,4/1,3,5-benzene products.

Methyl propargyl ether demonstrates a somewhat different reactivity from propiolates or phenylacetylene. Conversion of methyl propargyl ether also depends on the reaction conditions: only 25% of the starting material reacts after 24 h at RT with 1 mol% catalyst present, while increasing the reaction temperature to 50 °C increases conversion rate to 49%. Consistent with our previous observations (for ethyl propiolate), catalysis at 1 mol% produces mixtures of benzenes and cyclooctatetraenes. However, in contrast to the reactivity of propiolates and phenylacetylene, cyclooctatetraenes are the dominant product under these conditions for methyl propargyl ether. At 1 mol% catalyst and 50 °C, approximately 75% of the product constitutes cyclooctatetraenes, as determined by <sup>1</sup>H NMR spectroscopy and GC-MS. Interestingly, and in agreement with the results observed for propiolates and phenyl acetylene, the reaction at 5 mol% catalyst and room temperature produces benzene products exclusively. For cyclopropylacetylene, only relatively low conversion was detected; no reactivity with trimethylsilylacetylene was observed.

**Table 1.** Reactivity of complex **2** in cyclotrimerisation reactions with terminal alkynes. All reactions were carried out for 24 h, after which the nature of the products was determined by  $^1\text{H}$  NMR spectroscopy and GC-MS.



R	solvent	mol %	T	% conversion	Benzenes % 1,2,4 / % 1,3,5	Combined cyclooctatetraenes (%)
	$\text{C}_6\text{D}_6$	1	RT	89	56 / 12	21
	$\text{C}_6\text{D}_6$	5	RT	100	75 / 25	0
	Ether	1	RT	nd <sup>a</sup>	28 / 7	nd
	THF	1	RT	nd <sup>a</sup>	27 / 5	nd
	$\text{CH}_3\text{CN}$	1	RT	nd <sup>a</sup>	22 / 23	0
	$\text{C}_6\text{D}_6$	1	RT	94	48 / 10	36
	$\text{C}_6\text{D}_6$	5	RT	96	82 / 14	<1
	$\text{C}_6\text{D}_6$	1	RT	27	10 / 4	13
	$\text{C}_6\text{D}_6$	1	50 °C	49	9 / 4	36
	$\text{C}_6\text{D}_6$	5	RT	44	29 / 15	0
	$\text{CH}_3\text{CN}$	5	RT	nd <sup>a</sup>	9 / 4	nd
	$\text{C}_6\text{D}_6$	1	RT	32	25 / 8	0
	$\text{C}_6\text{D}_6$	5	RT	44	33 / 11	0
	$\text{C}_6\text{D}_6$	5	50 °C	92	70 / 22	0
	$\text{C}_6\text{D}_6$	1	RT	8	6 / 2	0
	$\text{C}_6\text{D}_6$	1	50 °C	18	15 / 3	0
	$\text{C}_6\text{D}_6$	1	RT	<1	- / -	-

nd = Not determined. <sup>a</sup>We were not able to determine % conversion as volatiles had to be removed prior to dissolving the reaction mixture in deuterated solvents.

We note that cycloaddition reactions of various terminal alkynes using related mononuclear diazadiene and iminopyridine nickel(0) precursors has been reported by several

groups.<sup>13, 24</sup> For these complexes, the cycloaddition reaction often takes the cyclotetramerisation route preferably. tom Dieck and coworkers demonstrated selective cyclotetramerisation of several different mono-substituted alkynes by a diazadiene nickel precursors,<sup>24</sup> among them ethyl and methyl propiolates.<sup>24d</sup> Uyeda and coworkers demonstrated that a mononuclear iminopyridine nickel(0) complex (**14**, **Figure 5**) catalyses alkyne cycloaddition reactions of ethyl propiolate and phenylacetylene.<sup>13</sup> Specifically for ethyl propiolate substrate, mononuclear iminopyridine nickel catalyst forms cyclooctatetraenes primarily (>70%); the combined yield of benzene products (both 1,2,4- and 1,3,5 regioisomers) was only around 20%, and the total substrate conversion was slightly higher than 30%. A related mononuclear bipyridine-nickel catalyst (**15**, **Figure 5**) showed similar reactivity: ca. 30% total conversion, of which cyclooctatetraenes constituted the majority of the product. Under the same reaction conditions, Uyeda's dinuclear catalyst (**13**, **Figure 5**) formed mostly benzenes (in ca. 90% yield).

To evaluate the effect of metal-metal cooperativity engendered by our  $[\text{Ni}_2(\text{L})]$  system, we decided to directly compare its cycloaddition reactivity with the reactivity of mononuclear and dinuclear nickel iminopyridine/naphthyridine complexes reported by Uyeda and coworkers (**Figure 5**), using identical reaction conditions. Accordingly, we carried out catalytic experiments under reaction conditions identical to these used by Uyeda and coworkers for ethyl propiolate (22 °C, 11 min, 1 mol % catalyst), and phenylacetylene (60 °C, 40 min, 5 mol% catalyst). The results are described in **Table 2** below. For ethyl propiolate, our catalyst enables 46% conversion after 11 min; benzenes constitute nearly 80% of the product (1,2,4:1,3,5 ratio of 4:1). Similar results were obtained for phenylacetylene: our system forms benzenes exclusively. These experiments clearly support metal-metal cooperativity in our catalyst, as all related mononuclear

catalysts (with iminopyridine, bipyridine or diazadiene ligands) form primarily cyclooctatetraenes.

**Table 2.** Comparison between the catalytic reactivity of complex **2** with the previously reported mononuclear and dinuclear compounds. Reaction conditions for ethyl propiolate: 22 °C, 11 min, 1 mol% catalyst. Reaction conditions for phenylacetylene: 60 °C, 40 min, 5 mol% catalyst. Structures of the mononuclear precatalysts (other than complex **2**) is given in **Figure 5** below; their synthesis and reactivity is reported in ref. 13.

R	catalyst	% conversion	Benzenes % 1,2,4 / % 1,3,5	Combined cyclooctatetraenes (%)
	2	46	28 / 7	11
	13	100	68 / 22	10
	14	33	6 / 2	25
	15	32	12 / 2	18
	2	64	59 / 5	0
	13	100	97 / 3	0
	14	53	24 / 4	25
	15	40	12 / 4	24

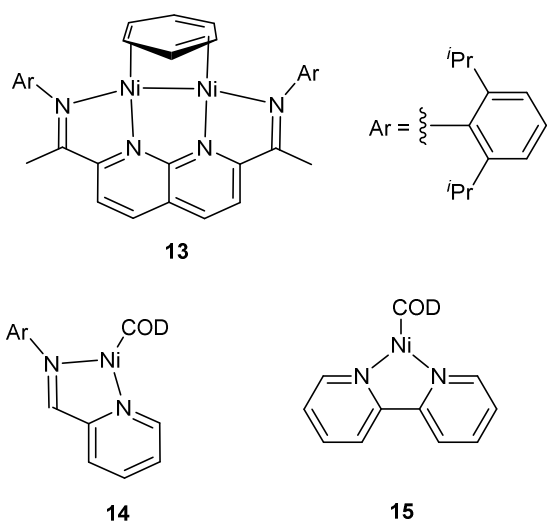


**Figure 5.** Structures of pre-catalysts in **Table 2**.

## DFT Analysis of Reaction Mechanism

To understand the cyclotrimerisation observed experimentally, we mapped the reaction path for **4** with additional equivalents of acetylene. This model was chosen to minimize the numerous regioisomers and rotamers involved in the mechanism of the substituted alkynes. Free energies are based on B3LYP/6-311+G(d,p) single point refinements at the B3LYP/6-31G(d) optimized geometries (see Computational Methods for full details). Binding of a second acetylene results in a 90-degree twist of the first alkyne relative to the mono-alkyne adduct (**Figure 6**). This dialkyne adduct, **7**, is computed to be 23.78 kcal/mol higher in energy and shows similar intraligand bonding in the iminopyridine as the monoalkyne adducts. However, the Ni centers no longer have unpaired spins; the species is best described as a closed-shell singlet.

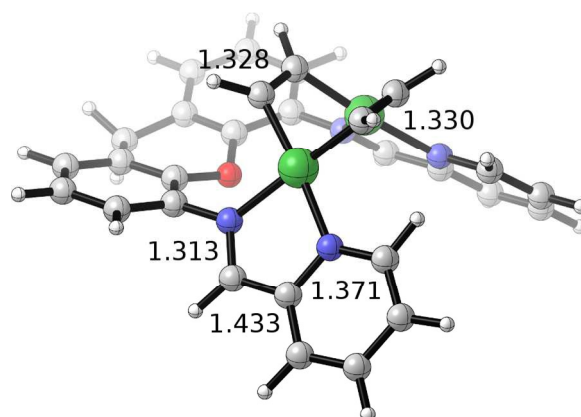


**Figure 6.** Optimized structure of the di-alkyne adduct **7** with important bond lengths (Å) labeled. Images generated in CYLview.<sup>21</sup>

Bond elongation in both alkynes of 1.33 Å (vs. 1.21 Å for free acetylene) is only slightly less than the value of 1.37 Å for **1**. Coupling of these activated alkynes to afford a nickelacyclopentadiene (**8**) has a barrier of only 3.49 kcal/mol relative to **7**, or 27.27 kcal/mol relative to **4**. The structure of this transition state (**7-8-TS**) is shown in **Figure 7** (left). After surmounting this barrier, an extremely stable nickelacyclopentadiene is formed (−27.54 kcal/mol

vs. **4** and free acetylene). As shown in **Figure 7** (right), the nickelacycle is  $\eta^4$ -bound to the second nickel center. This computed structure is similar to previously described ditungsten,<sup>8</sup> dicobalt,<sup>12</sup> and ditantalum species<sup>9</sup>, and contrasts with the  $\eta^2$  coordination of the nickelacyclopentadiene in Uyeda's dinickel system.<sup>13</sup>

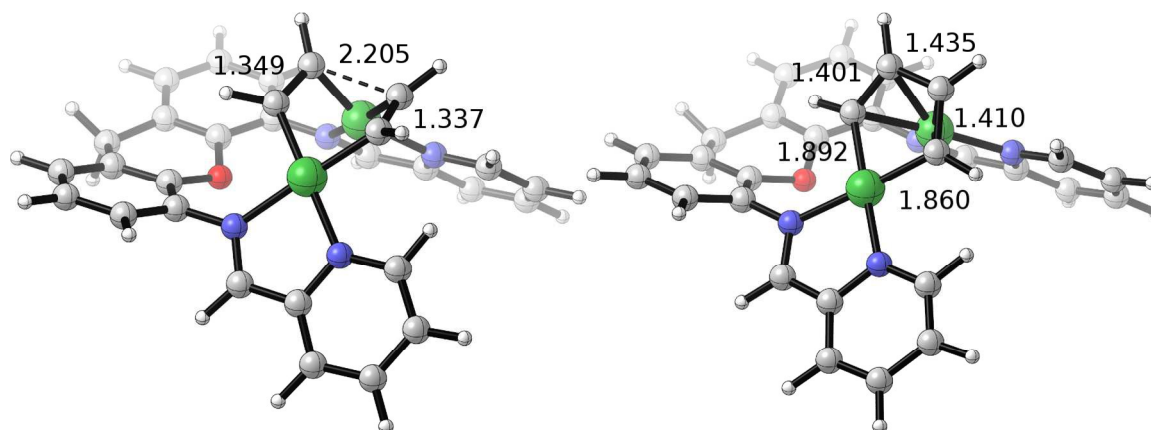


**Figure 7.** Optimized structure of **7-8-TS** (left) and **8** (right) with important bond lengths (Å) labeled. Images generated in CYLview.<sup>21</sup>

From intermediate **8**, we explored the hypothesized [4 + 2] and alkyne insertion pathways. No transition states or intermediates corresponding to a [4 + 2] cycloaddition or transition state for direct insertion were located. [2 + 2] addition products to both Ni–C bonds afforded intermediates **9a** and **9b** (**Figure 8**) with relative energies of 6.35 and 7.38 kcal/mol, respectively. **9a** and **9b** differ in whether the newly formed nickelacyclobutene is syn or anti to the xanthene in the dinucleating ligand backbone. In principle, addition could occur from the bottom face of the complex as well, however, both of these regioisomers, **9c** and **9d**, were computed to be much more endergonic at 16.21 and 47.63 kcal/mol (see SI Figure S48).

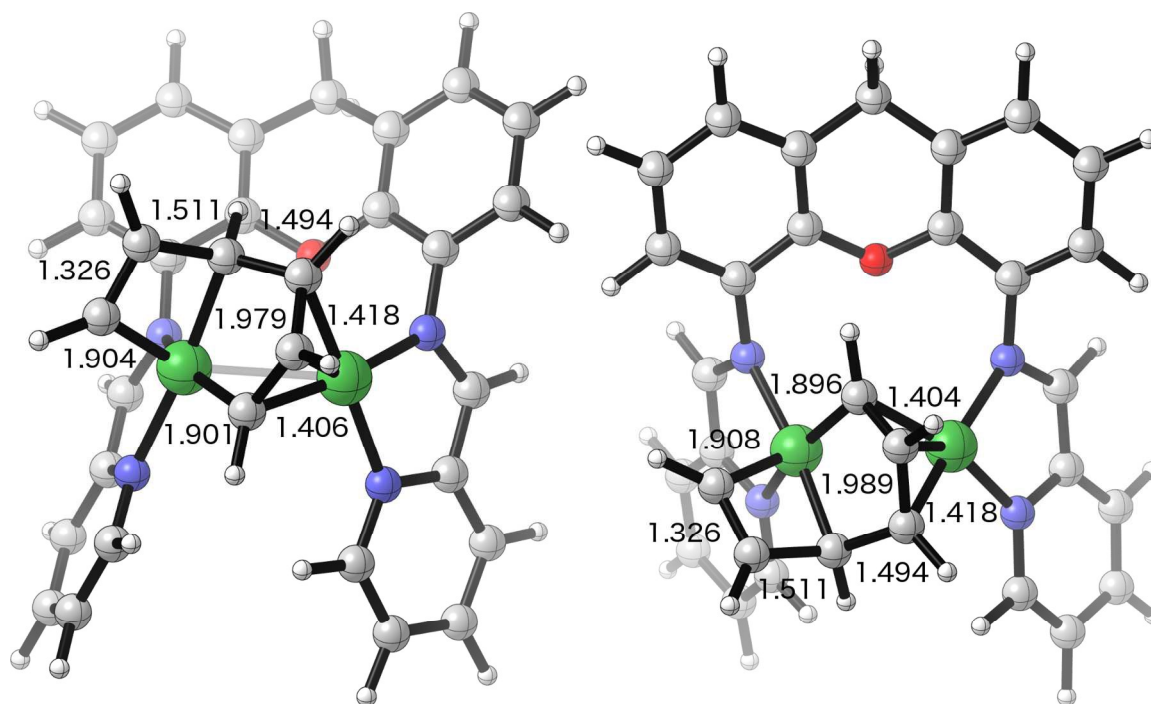


**Figure 8.** Top-down views of the fused nickelabicycles optimized structures of **9a** and **9b** with important bond lengths (Å) labeled. Images generated in CYLview.<sup>21</sup>

As **Figure 8** shows, bonding within the fused nickelabicycles of **9a** and **9b** is quite similar, with the largest deviations in the Ni–C contacts ( $\sim 0.005$  Å). In both structures, the five-membered ring remains  $\eta^3$ -bound to the second Ni ion. Despite the slight thermodynamic preference for **9a** vs. **9b**, the corresponding cycloaddition barriers are 28.75 and 22.53 kcal/mol, respectively (see SI Figure S49 for **8-9a-TS** and **8-9b-TS** structures). Thus, we focused further reaction analysis on regioisomer **9b**, based on this kinetic preference.

Elongation of the Ni–C bond in this intermediate relieves ring strain and affords **10**, a nickelacycloheptatriene. The transition state for this ring expansion, **9b-10-TS** (**Figure 9**, left), has similar bonding within the metallacycle other than the significantly elongated Ni–C bond from 1.989 to 2.317 Å. Similar to **8** that featured two short and one long C–C bond lengths, **10** has alternating short and long bond lengths suggesting three  $\pi$  bonds in this metallacycle (**Figure**

**9**, right). Importantly, the ring maintains  $\eta^3$ -coordination, seen in both **9b** and **9b-10-TS**, within this intermediate. Because of this, the ring is concave toward the two Ni centers, causing the hydrogens not involved in haptic binding to the second Ni to pucker above the ring.

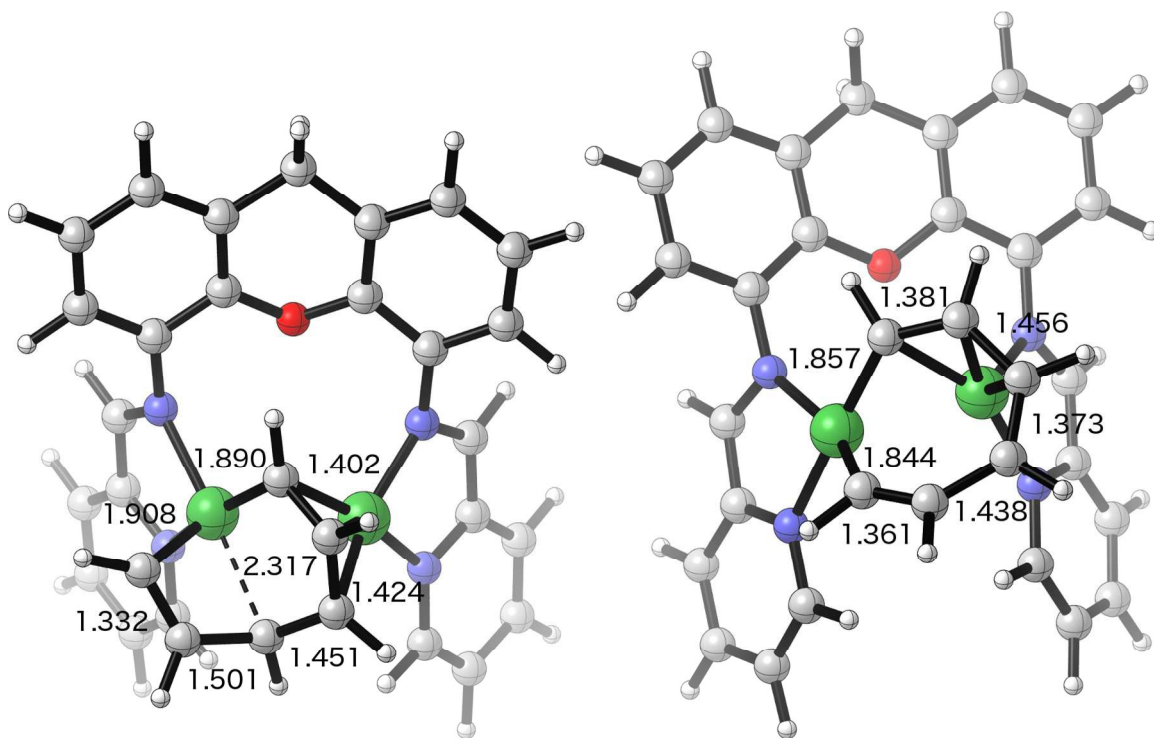


**Figure 9.** Optimized structure of **9b-10-TS** (left) and **10** (right) with important bond lengths (Å) labeled. Images generated in CYLview.<sup>21</sup>

The barrier for **9b-10-TS** is only 0.41 kcal/mol higher in energy than **9b**, suggesting the ring expansion is effectively barrierless. **10** is exergonic by 27.35 kcal/mol vs. **8** and acetylene. Reductive elimination of benzene from **10** is facile with a barrier of only 1.64 kcal/mol; however, this reductive elimination requires a conformational change to the xanthene backbone (**10'**, see Supporting Information Figure S50). This conformer is computed to be slightly more stable (−0.63 kcal/mol) than **10**.

To explore the origin of the COT isomers observed experimentally, nickelacyclononatetraene **11** was optimized (**Figure 10**). All attempts to find the barrier for [2 + 2] addition of acetylene to **10** resulted in COT-coordinated species **12** (−36.97 kcal/mol vs. **10** and acetylene) rather than barriers to intermediate **11**.

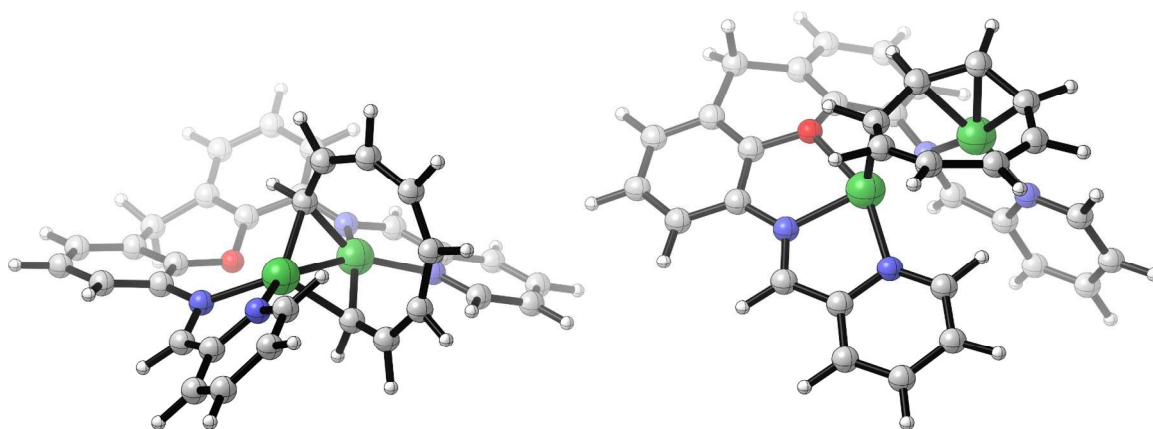


**Figure 10.** Optimized structures of **11** (left) and **12** (right). Images generated in CYLview.<sup>21</sup>

**11** is thermodynamically competitive with intermediate **10**, being only 0.83 kcal/mol uphill; however, the low-barrier process to eliminate benzene makes this species difficult to rationalize kinetically, unless alkyne insertion is essentially barrierless. As mentioned before, the ring puckering of the nickelacycloheptatriene in **10** may hinder the approach of the incoming alkyne, since the most accessible face of the Ni–C bonds is from below (where we observed unfavorable thermodynamics in intermediates **9c** and **9d**). Work is ongoing to map out the transformation from **10** to **12**, and to probe the regioisomers and rotamers accessible in the ester- and ether-substituted species. Due to steric congestion in the dinickel pocket, it is possible that significant structural changes will occur in the nickelacycles once substituted alkynes are used, opening the way for COT formation.

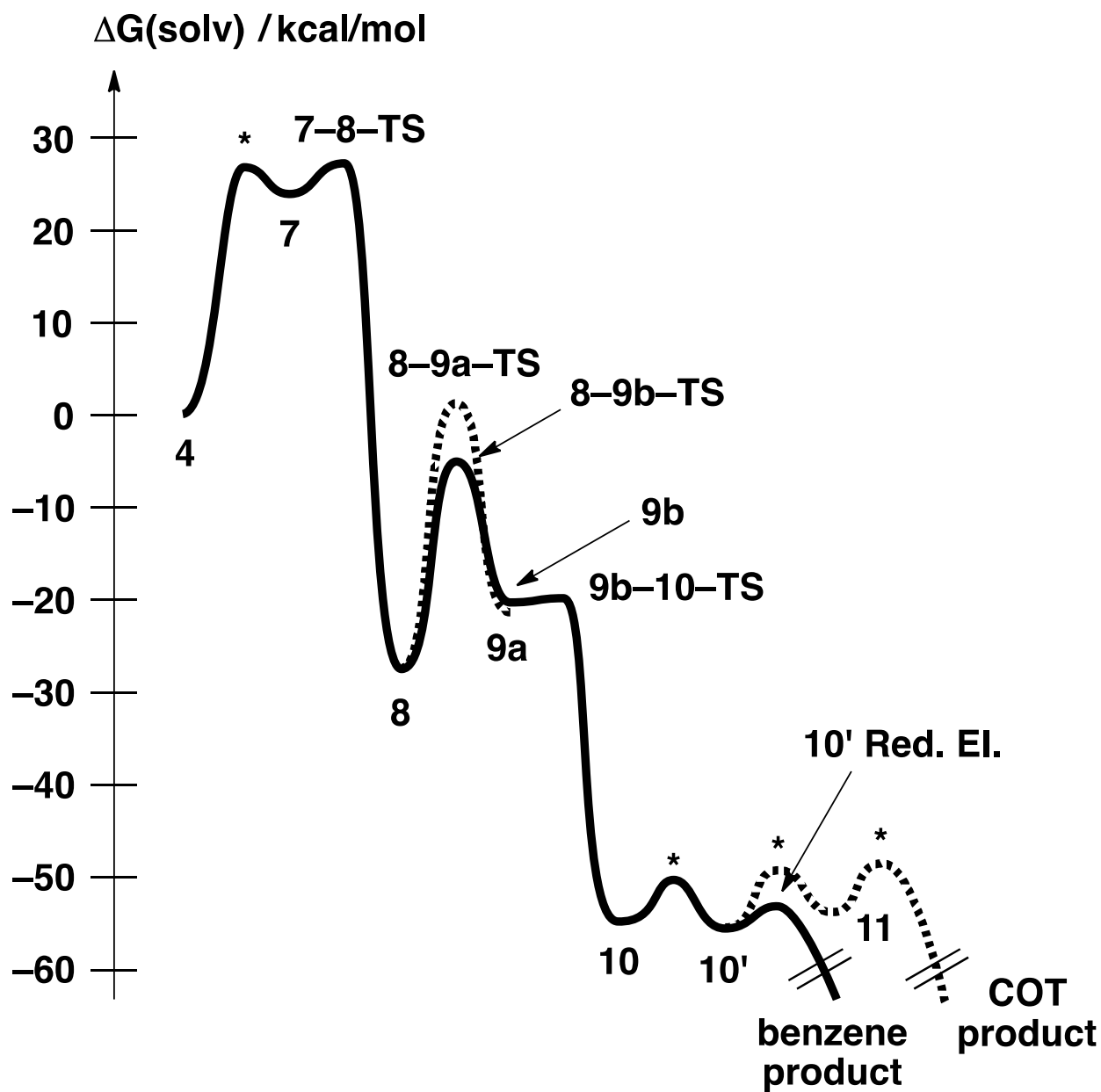


**Figure 11.** Reaction profile for the production of benzene and cyclooctatetraenes with HCCH. Intermediates 9c and 9d, which were determined to be much higher in energy, were excluded for clarity. Transition states that were not explicitly located are labeled with \*.

**Figure 11** summarizes the thermodynamics and kinetics for the intermediates and transition states presented in **Figures 6-10**. Based on this simplified alkyne model (HCCH), cyclization to

form the nickelacyclopentadiene intermediate **8** is rate-determining with  $\Delta G^\ddagger = 27.27$  kcal/mol. The subsequent [2+2], ring expansion, and reductive elimination steps should be facile in comparison with  $\Delta G^\ddagger$  of 22.53, 16.21, and 1.64 kcal/mol, respectively. This may explain our inability to isolate intermediate **8** like Uyeda,<sup>13</sup> but it is important to caution that these energetics may change significantly once the alkyne substituents are included. Computational work is ongoing to better understand the regioselectivity of this system.

### Summary and Conclusions

A new dinickel complex ligated by a semi-rigid xanthene-bridged bis(iminopyridine) dinucleating ligand serves as a catalyst for cycloaddition of various terminal alkynes. Relatively high conversion rates ( $\geq 90\%$ ) are observed for alkyl propiolates using low catalyst loading (1 mol%) at room temperature. For phenyl acetylene and methyl propargyl ether, heating and/or higher catalyst loading are required to achieve comparable conversion rates during the same reaction runtime. With alkyl propiolates and phenyl acetylene, efficient cyclotrimerisation is obtained, giving 1,2,4-isomers predominantly. While significant amount of cyclotetramerisation was observed with methyl propargyl ether, it occurs only at low catalyst concentration (1 mol%). At higher catalyst concentration (5 mol%), this substrate also forms benzenes exclusively. A direct comparison (using identical reaction conditions) with related dinuclear (diiminonaphthyridine) or mononuclear (iminopyridine, diazadiene, bipyridine) catalysts indicated that our system, similarly to the previously reported diiminonaphthyridine also exhibits bimetallic cooperativity which enables it to preferentially form benzene products.. There are, however, several notable differences between the present system and the diiminonaphthyridine (Uyeda's) system. While both systems appear to retain their dinuclear composition throughout catalysis, diiminonaphthyridine system demonstrates a significantly faster reaction rates, and

somewhat higher selectivity for cyclotrimerisation. We hypothesize that the reactivity differences stem from the different flexibility of the catalysts. Diiminonaphthyridine positions two nickel centers side by side, in a rigid arrangement that subsequently allows little flexibility in the nickel-nickel distance. In contrast, our xathene-based bis(iminopyridine) allows relatively flexible nickel-nickel distance. Of course, two mononuclear nickel complexes allow the “ultimate” flexibility in nickel-nickel distance, if bimetallic intermediates/transition states are invoked for monometallic precursors.<sup>24</sup> This flexibility can then be correlated with the catalyst selectivity in the formation of benzenes vs. cyclooctatetraenes, as the intermediates/transition states for cyclooctatetraenes require wider range of metal-metal distances (2.38 – 2.77 Å) vs. benzenes (2.51 – 2.65 Å), according to DFT calculations. Due to the constrained nature of the Uyeda’s system with the “fixed” nickel-nickel distance, it shows a profound preference towards cyclotrimerisation. A bimetallic complex made of two independent nickel centers as in Tom Dieck’s work<sup>24</sup> can accommodate wider range of nickel-nickel distances, thus leading to cyclooctatetraenes. Our complex, while being relatively rigid, is not as constrained as Uyeda’s, and therefore leads preferentially to benzenes, but not as efficiently. It should be cautioned that all calculations were performed on a model system in both the ligand backbone and the alkyne, and future work will explore the role of each simplification on the proposed mechanistic pathway. Future experimental studies will focus on the synthesis of bimetallic complexes in more rigid ligand environments, the exploration of their reactivity, and the attempted isolation of key metallacycle intermediates predicted by DFT.

## Experimental

*General Methods and Procedures.* All reactions involving air-sensitive materials were executed in a nitrogen-filled glovebox. Diphenylacetylene, ethyl propiolate, methyl propargyl ether, phenylacetylene, ethynyltrimethylsilane, and hexamethylbenzene were purchased from Aldrich. *tert*-Butyl propiolate was purchased from Alfa Aesar. Bis(cyclooctadiene)nickel(0) was purchased from Strem. All chemicals were used as received. The synthesis of the ligand and  $\text{Ni}_2(\text{DPA})(\text{COD})_2$  were previously reported.<sup>1, 2</sup> All non-deuterated solvents were purchased from Aldrich and were of HPLC grade. The non-deuterated solvents were purified using an MBraun solvent purification system. Benzene- $\text{d}_6$  was purchased from Cambridge Isotope Laboratories. All solvents were stored over 3 Å molecular sieves. Compounds were generally characterized by  $^1\text{H}$  and  $^{13}\text{C}$  NMR, X-ray crystallography, elemental analysis, gas chromatography-mass spectrometry, and electrospray ionization mass spectrometry. NMR spectra were recorded at the Lumigen Instrument Center (Wayne State University) on an Agilent 400 MHz Spectrometer in  $\text{C}_6\text{D}_6$  at room temperature. Chemical shifts and coupling constants ( $J$ ) were reported in parts per million ( $\delta$ ) and Hertz respectively. Elemental analysis was performed under ambient, air-free conditions by Midwest Microlab LLC.

*Preparation of 2 from  $\text{Ni}_2(\text{DPA})(\text{COD})_2$  (I).* A 2 mL hexane solution of  $\text{Ni}_2(\text{DPA})(\text{COD})_2$  (102.4 mg, 0.200 mmol) and a 2 mL THF solution of the ligand (106.1 mg, 0.200 mmol) were prepared and cooled to  $-35\text{ }^\circ\text{C}$ . The ligand was added dropwise to a stirring solution of  $\text{Ni}_2(\text{DPA})(\text{COD})_2$ . Over the next 15 minutes, black precipitate formed and the solution color changed to brown. The reaction was stirred for 2 hours, upon which the volatiles were removed in vacuo. The resulting residue was dissolved in 5 mL of THF, covered with 10 mL of hexane, and allowed to stand for 24 hours at  $-35\text{ }^\circ\text{C}$ . The supernatant was removed, and the solid washed with hexane and dried in vacuo to afford black crystals (102.7 mg, 0.124 mmol, 62%). X-ray quality crystals were

obtained from a saturated ether solution of **2** at -35 °C.  $^1\text{H}$  NMR ( $\text{C}_6\text{D}_6$ , 400 MHz)  $\delta$  11.31 (d,  $J = 8.0$  Hz, 2H,  $\beta\text{-H}$  on pyridine), 9.50 (s, 2H, imino-**H**), 8.06 (d,  $J = 12.0$  Hz, 2H, ortho-**H** on phenylacetylene), 7.61 (d, 2H,  $J = 1.0$  Hz, ortho-**H** on xanthene), 7.35 (d,  $J = 8.0$  Hz, 2H, ortho-**H** on phenylacetylene), 7.31 (t,  $J = 4.0$  Hz, 2H,  $\gamma\text{-H}$  on pyridine), 7.15-7.25 (t + t, 2H + 2H,  $\beta\text{-H}$  on pyridine + meta-**H** on phenylacetylene), 7.15 (d, 2H, para-**H** on xanthene – hidden by benzene), 7.08 (t,  $J = 8.0$  Hz, 1H, para-**H** on phenylacetylene), 6.89 (t,  $J = 8.0$  Hz, 1H, para-**H** on phenylacetylene), 6.79 (t,  $J = 8.0$  Hz, 2H, meta-**H** on phenylacetylene), 6.62 (d,  $J = 8.0$  Hz, 2H,  $\alpha\text{-H}$  on pyridine), 2.02 (s, 3H, methyl-**H**), 1.61 (s, 3H, methyl-**H**), 1.37 (s, 18H, tert-butyl-**H**);  $^{13}\text{C}\{^1\text{H}\}$  NMR ( $\text{C}_6\text{D}_6$ , 400 MHz)  $\delta$  155.86, 153.85, 147.20, 146.64, 145.06, 145.00, 142.92, 141.68, 133.02, 130.69, 130.20, 129.16, 128.78, 127.29, 126.40, 124.35, 123.38, 123.07, 121.92, 119.39, 94.70, 89.36, 37.14, 35.94, 34.91, 32.15, 27.90, 23.99, 14.69. Anal. Calcd for  $\text{C}_{49}\text{H}_{48}\text{N}_4\text{Ni}_2\text{O}$ : C, 71.22; H, 5.86; N, 6.78. Found: C, 70.99; H, 6.04; N, 6.50.

*One-Pot Preparation of 2.* A 2 mL hexane solution of diphenylacetylene (39.2 mg, 0.220 mmol) was added dropwise to a 2 mL hexane solution of  $\text{Ni}(\text{COD})_2$  (110.0 mg, 0.400 mmol). Over the next 15 minutes, dark red precipitate formed and the solution color changed to red. The reaction was stirred for 2 hours and then cooled to -35 °C. A 2 mL THF solution of the ligand (106.1 mg, 0.200 mmol) cooled to -35 °C was then added dropwise to the stirred solution of diphenylacetylene and  $\text{Ni}(\text{COD})_2$ . Over the next 15 minutes, black precipitate formed and the solution color changed to brown. The reaction was stirred for 2 hours, upon which the volatiles were removed in vacuo. The resulting residue was dissolved in 5 mL of THF, covered with 10 mL of hexane, and allowed to stand for 24 hours at -35 °C. The supernatant was removed, and the solid washed with hexane and dried in vacuo to afford black crystals (149.3 mg, 0.181 mmol, 90%).

*Preparation of 3 from 2.* A 0.12 mL aliquot of a 0.247 M solution of ethyl propiolate in C<sub>6</sub>D<sub>6</sub> (0.030 mmol) was added dropwise to a 2 mL C<sub>6</sub>D<sub>6</sub> solution of **2** (24.8 mg, 0.030 mmol). Immediately, the solution color adopted a slight green tinge. The reaction was stirred for 1 hour, upon which volatiles were removed in vacuo. The residue was washed with 5 mL of ether and dried in vacuo to afford a black solid (19.1 mg, 0.026 mmol, 85%). <sup>1</sup>H NMR (C<sub>6</sub>D<sub>6</sub>, 400 MHz) δ 11.99 (d, *J* = 4.0 Hz, 2H, β-**H** on pyridine), 9.24 (s, 2H, imino-**H**), 7.71 (d, *J* = 4.0 Hz, 2H, ortho-**H** on xanthene), 7.43 (t, *J* = 6.0 Hz, 2H, γ-**H** on pyridine), 7.19 (d, *J* = 2.0 Hz, 2H, para-**H** on xanthene), 7.12 (t, *J* = 8.0 Hz, 2H, β-**H** on pyridine), 6.59 (d, *J* = 8.0 Hz, 2H, α-**H** on pyridine), 4.26 (q, *J* = 8.0 Hz, 2H, methylene-**H** on ethyl propiolate), 3.83 (s, 1H, acetylene-**H**), 2.09 (s, 3H, methyl-**H** on xanthene), 1.69 (s, 3H, methyl-**H** on xanthene), 1.36 (s, 18H, tert-butyl-**H**), 1.03 (t, *J* = 8.0 Hz, 3H, methyl-**H** on ethyl propiolate); <sup>13</sup>C{<sup>1</sup>H} NMR (C<sub>6</sub>D<sub>6</sub>, 400 MHz) δ 167.79, 155.69, 154.68, 149.32, 146.63, 144.71, 133.24, 131.52, 125.72, 124.26, 122.11, 120.09, 75.97, 68.73, 59.69, 36.87, 36.24, 34.95, 32.08, 28.80, 15.19. Anal. Calcd for C<sub>40</sub>H<sub>44</sub>N<sub>4</sub>Ni<sub>2</sub>O<sub>3</sub>×C<sub>4</sub>H<sub>10</sub>O: C, 64.42; H, 6.64; N, 6.83. Found: C, 64.97; H, 6.19; N, 6.32.

*Treatment of 2 with 2 equiv. of Ethyl propiolate.* A 0.24 mL aliquot of a 0.247 M solution of ethyl propiolate in C<sub>6</sub>D<sub>6</sub> (0.060 mmol) was added dropwise to a 2 mL C<sub>6</sub>D<sub>6</sub> solution of **2** (24.8 mg, 0.030 mmol). Immediately, the solution color adopted a slight green tinge. The reaction was stirred for 1 hour, upon which NMR spectra was obtained for the reaction mixture. Analysis of the spectra revealed the absence of a diadduct compound and the presence of **2** and cyclotrimerisation products.

*Treatment of 2 with 2 equiv. of Ethyl propiolate in the presence of internal standard (hexamethylbenzene).* A solution of ethyl propiolate (0.075 mmol) hexamethylbenzene (0.006 mmol) in C<sub>6</sub>D<sub>6</sub> with was added dropwise to a 2 mL C<sub>6</sub>D<sub>6</sub> solution of **2** (24.8 mg, 0.030 mmol).

Immediately, the solution color adopted a slight green tinge. The reaction was stirred for 1 hour, upon which NMR spectra was obtained for the reaction mixture. Analysis of the spectra revealed the absence of a diadduct compound and the presence of **3** (0.030 mmol) and cyclotrimerisation products (0.011 mmol of the 1,2,4-isomer and 0.003 mmol of the 1,3,5-isomer). For analyzing the presence of **3**, the peaks at 12.00 ppm and 9.24 ppm (2H and 2H respectively) were used. For analyzing the presence of the 1,3,5-isomer, the peak at 9.14 ppm (3H) was used. For analyzing the presence of the 1,2,4-isomer, the peaks at 8.63 ppm and 7.98 ppm (1H and 1H respectively) were used.

*Treatment of 2 with 1 equiv. of Methyl propargyl ether or Phenylacetylene.* A 0.10 mL aliquot of a 0.296 M solution of methyl propargyl ether in C<sub>6</sub>D<sub>6</sub> (0.030 mmol) or a 0.13 mL aliquot of a 0.228 M solution of phenylacetylene in C<sub>6</sub>D<sub>6</sub> (0.030 mmol) was added dropwise to a 2 mL C<sub>6</sub>D<sub>6</sub> solution of **2** (24.8 mg, 0.030 mmol). Immediately, the solution color adopted a slight green tinge. The reaction was stirred for 1 hour, upon which NMR spectra was obtained for the reaction mixture. Analysis of the spectra revealed the absence of a monoadduct compound and the presence of **2**, diphenylacetylene, cyclotrimerisation products, and unidentifiable compound(s).

*Treatment of 2 with 2 equivalents of Methyl propargyl ether or Phenylacetylene.* A 0.20 mL aliquot of a 0.296 M solution of methyl propargyl ether in C<sub>6</sub>D<sub>6</sub> (0.060 mmol) or a 0.26 mL aliquot of a 0.228 M solution of phenylacetylene in C<sub>6</sub>D<sub>6</sub> (0.060 mmol) was added dropwise to a 2 mL C<sub>6</sub>D<sub>6</sub> solution of **2** (24.8 mg, 0.030 mmol). Immediately, the solution color adopted a slight green tinge. The reaction was stirred for 1 hour, upon which NMR spectra was obtained for the reaction mixture. Analysis of the spectra revealed the absence of a monoadduct compound and the presence of **2**, diphenylacetylene, cyclotrimerisation products, and an unidentified compound.

*General Procedure for Catalytic Cyclotrimerisation Reactions (See Table 1).* A scintillation vial containing **2** (8.3 mg, 0.010 mmol) was treated with the appropriate amount of monosubstituted alkyne in a C<sub>6</sub>D<sub>6</sub> solution or another solvent of choice, with hexamethylbenzene as the internal integration standard. Immediately, the solution color changed to green. The reaction mixture was stirred for 24 hours at the appropriate temperature, upon which NMR spectra was obtained for the reaction mixture in C<sub>6</sub>D<sub>6</sub>. For reaction mixtures in other solvents, volatiles were removed in vacuo and the resulting residue was re-dissolved in C<sub>6</sub>D<sub>6</sub>. Analysis of the spectra revealed the quantitative presence or absence of cyclotrimerisation products. For selected reactions, an aliquot of the reaction mixture was analyzed by GC-MS for the quantitative presence of cyclooctatetraenes and benzenes.

**Electronic supplementary information** (ESI) available: NMR spectra, crystal and refinement data for compound **2**, and Cartesian coordinates and energetics for all calculated species. The crystallographic data in cif format for compound **2** was deposited at the Cambridge Crystallographic Data Centre under the following number: CCDC 1519915.

### Acknowledgements

SG thanks Wayne State University for the initial sponsorship of this project and the National Science Foundation (NSF) for current support under grant number CHE-1349048. RLL thanks the Research Corporation (Cottrell College Science Award) and the NSF for computational resources (CHE-1039925 to the Midwest Undergraduate Computational Chemistry Consortium). Compounds characterization was carried out at Lumigen Instrument Center at Wayne State University.

### References

1. (a) S. Saito and Y. Yamamoto, *Chem. Rev.* 2000, **100**, 2901. (b) P. Kumar and J. Louie, In *Transition-Metal-Mediated Aromatic Ring Construction*; K. Tanaka, Ed.; John Wiley & Sons, Inc.: Hoboken, NJ, 2013; pp. 37–70. (c) C. Wang and Z. Xi, *Chem. Commun.*, 2007, 5119-5133.
2. (a) R. Diercks, B. E. Eaton, S. Gürtzgen, S. Jalisatgi, A. J. Matzger, R. H. Radde and K. P. C. Vollhardt, *J. Am. Chem. Soc.*, 1998, **120**, 8247-8248; (b) D. R. McAlister, J. E. Bercaw and R. G. Bergman, *J. Am. Chem. Soc.*, 1977, **99**, 1666-1668; (c) D. P. Smith, J. R. Strickler, S. D. Gray, M. A. Bruck, R. S. Holmes and D. E. Wigley, *Organometallics*, 1992, **11**, 1275-1288; (d) O. V. Ozerov, F. T. Ladipo and B. O. Patrick, *J. Am. Chem. Soc.*, 1999, **121**, 7941-7942.
3. (a) M. O. Albers, D. J. A. De Waal, D. C. Liles, D. J. Robinson, E. Singleton and M. B. Wiege, *J. Chem. Soc., Chem. Commun.*, 1986, 1680-1682; (b) B. Hessen, A. Meetsma, F. van Bolhuis and J. H. Teuben, *Organometallics*, 1990, **9**, 1925-1936; (c) F. Calderazzo, G. Pampaloni, P. Pallavicini, J. Straehle and K. Wurst, *Organometallics*, 1991, **10**, 896-901.
4. For selected examples, see: (a) W. Reppe, O. Schlichting, K. Klager and T. Toepel, *Justus Liebigs Ann. Chem.*, 1948, **560**, 1-92; (b) P. Alphonse, F. Moyon and P. J. Mazerolles, *J. Organomet. Chem.* 1988, **345**, 209-216; (c) P. Bicev, A. Furlani and G. Sartori, *Gazz. Chim. Ital.* 1973, **103**, 849-858; (d) S. K. Rodrigo, I. V. Powell, M. G. Coleman, J. A. Krause and H. Guan, *Org. Biomol. Chem.*, 2013, **11**, 7653-7657; (e) C. Xi, Z. Sun and Y. Liu, *Y. Dalton Trans.* 2013, **42**, 13327-13330.
5. K. Yamamoto, H. Nagae, H. Tsurugi and K. Mashima, *Dalton Trans.*, 2016, **45**, 17072-17081.
6. (a) F. A. Cotton, W. T. Hall, K. J. Cann and F. J. Karol, *Macromolecules*, 1981, **14**, 233-236; (b) F. A. Cotton and W. T. Hall, *Inorg. Chem.*, 1981, **20**, 1285-1287.
7. (a) M. Kakeya, T. Fujihara, T. Kasaya and A. Nagasawa, *Organometallics*, 2006, **25**, 4131-4137; (b) M. Matsuura, T. Fujihara, M. Kakeya, T. Sugaya and A. Nagasawa, *J. Organomet. Chem.*, 2013, **745**, 288-298.
8. (a) M. H. Chisholm, B. W. Eichhorn, K. Folting and J. C. Huffman, *Organometallics*, 1989, **8**, 49-66; (b) M. H. Chisholm, B. W. Eichhorn, K. Folting and J. C. Huffman,

- Organometallics*, 1989, **8**, 67-79; (c) M. H. Chisholm, B. W. Eichhorn and J. C. Huffman, *Organometallics*, 1989, **8**, 80-89.
9. (a) K. Yamamoto, H. Tsurugi and K. Mashima, *Organometallics*, 2016, **35**, 1573-1581; (b) K. Yamamoto, H. Tsurugi and K. Mashima, *Chem. – Eur. J.*, 2015, **21**, 11369-11377.
10. (a) H.-Z. Chen, S.-C. Liu, C.-H. Yen, J.-S. K. Yu, Y.-J. Shieh, T.-S. Kuo and Y.-C. Tsai, *Angew. Chem., Int. Ed.*, 2012, **51**, 10342-10346; (b) Y. Chen and S. Sakaki, *Dalton Trans.*, 2014, **43**, 11478-11492.
11. W. Hübel and C. Hoogzand, *Chem. Ber.*, 1960, **93**, 103-115.
12. (a) G. R. Knox and M. D. Spicer, *Organometallics*, 1999, **18**, 197-205; (b) G. R. Knox and M. D. Spicer, *Organometallics*, 1999, **18**, 206-214.
13. S. Pal and C. Uyeda, *J. Am. Chem. Soc.*, 2015, **137**, 8042-8045.
14. (a) A. Bheemaraju, R. L. Lord, P. Müller and S. Groysman, *Organometallics*, 2012, **31**, 2120-2123; (b) A. Bheemaraju, J. W. Beattie, R. L. Lord, P. D. Martin and S. Groysman, *Chem. Commun.*, 2012, **48**, 9595-9597; (c) A. Bheemaraju, J. W. Beattie, E. G. Tabasan, P. D. Martin, R. L. Lord and S. Groysman, *Organometallics*, 2013, **32**, 2952-2962; (d) J. W. Beattie, D. S. White, A. Bheemaraju, P. D. Martin and S. Groysman, *Dalton Trans.*, 2014, **49**, 7979-7986; (e) R. Narayanan, M. McKinnon, B. R. Reed, K. T. Ngo, S. Groysman and J. Rochford, *Dalton Trans.*, 2016, **45**, 15285-15289; (f) A. Bheemaraju, J. W. Beattie, Y. Danylyuk, J. Rochford and S. Groysman, *Eur. J. Inorg. Chem.*, 2014, **34**, 5865-5873.
15. V. W. Day, S. S. Abdel-Meguid, S. Dabestani, M. G. Thomas, W. R. Pretzer and E. L. Muetterties, *J. Am. Chem. Soc.*, 1976, **98**, 8289-8291.
16. B. R. Reed, R. L. Lord, M. McKinnon, J. Rochford and S. Groysman, *Organometallics*, In Revision.
17. See Supplementary Information for full details: (a) S. H. Vosko, L. Wilk, and M. Nusair, *Can. J. Phys.*, 1980, **58**, 1200-1211; (b) C. Lee, C. W. Yang and R. G. Parr, *Phys. Rev. B*, 1988, **37**, 785-789; (c) A. D. Becke, *Phys. Rev. A*, 1988, **38**, 3098; (d) A. D. Becke, *J. Chem. Phys.*, 1993, **98**, 1372-1377; (e) P. J. Stephens, F. J. Devlin, C. F. Chabalowski and M. J. Frisch, *J. Chem. Phys.*, 1994, **98**, 11623-11627.
18. F. J. Neese, *Phys. Chem. Solids*, 2004, **65**, 781-785.

19. GaussView, Version 5.0.9, Dennington, Roy; Keith, Todd; Millam, John. Semichem Inc., Shawnee Mission, KS, 2009.
20. C. C. Lu, E. Bill, T. Weyhermüller, E. Bothe and K. Wieghardt, *J. Am. Chem. Soc.*, 2008, **130**, 3181-3197.
21. CYLview, 1.0b; Legault, C. Y. Université de Sherbrook, 2009 (<http://www.cylview.org>).
22. R. A. Haley, A. R. Zellner, J. A. Krause, H. Guan and J. Mack, *ACS Sustainable Chem. Eng.*, 2016, **4**, 2464-2469.
23. J. E. Hill, G. Balaich, P. E. Fanwick and I. P. Rothwell, *Organometallics*, 1993, **12**, 2911.
24. (a) R. Diercks, L. Stamp and H. tom Dieck, *Chem. Ber.*, 1984, **117**, 1913-1919; (b) H. tom Dieck, A. M. Lauer, L. Stamp and R. Diercks, *J. Mol. Catal.*, 1986, **35**, 317-328; (c) R. Diercks and H. tom Dieck, *Chem. Ber.*, 1985, **118**, 428-435; (d) H. tom Dieck and J. Dietrich, *Angew. Chem., Int. Ed. Engl.*, 1984, **23**, 893-894.

**Textual abstract**

A new di-nickel complex supported by a relatively flexible xanthene-bridged bis(iminopyridine) ligand is reported and its reactivity in alkyne cycloaddition is investigated.

**Graphical abstract**